

Transient Characteristics of β -Ga₂O₃ Nanomembrane Schottky Barrier Diodes on Various Substrates

Junyu Lai¹, Jung-Hun Seo¹, *

¹ Department of Materials Design and Innovation, University at Buffalo, The State University of New York, Buffalo, NY USA 14260.

E-mail: junghuns@buffalo.edu

Received xxxxxx

Accepted for publication xxxxxx

Published xxxxxx

Abstract

In this paper, a transient delayed rising and fall time of β -Ga₂O₃ NMs Schottky barrier diodes (SBDs) formed on four different substrates (diamond, Si, sapphire, and polyimide) were measured using a sub-micron second resolution time-resolved electrical measurement system under a different temperature condition. The devices exhibited noticeably less-delayed turn-on/off- the transient time when β - Ga₂O₃ NMs SBDs were transfer-printed on a high-k substrate. Furthermore, a relationship between the β - Ga₂O₃ NM thicknesses and their transient characteristics were systematically investigated and found that phonon scattering plays an important role in heat dissipation as the thickness of β - Ga₂O₃ NMs get thinner which is also verified by the Multiphysics simulator. Overall, our result reveals the impact of various substrates with different thermal properties and different β - Ga₂O₃ NMs thickness with the performance of β - Ga₂O₃ NMs based devices. Hence, these results can guide further efforts us to optimize the performance of future β - Ga₂O₃ devices by maximizing heat dissipation from the β -Ga₂O₃ layer.

Keywords: β - Ga₂O₃ nanomembrane diode, heat dissipation, transient characteristic

1. Introduction

Beta gallium oxide (β -Ga₂O₃) has attracted considerable attention as a next-generation wide-bandgap semiconductor for power device applications, high-frequency devices, and solar-blind photodetectors due to its superior material properties [1, 2], such as an ultrawide bandgap value (>4.8 eV), good carrier mobility (>300 cm²v⁻¹s⁻¹), and critical breakdown electric field (\approx 8 MV cm⁻¹)[3, 4]. To date, several β -Ga₂O₃ based field-effect transistors, gigahertz range RF amplifiers, and solar-blind Schottky diodes have been successfully demonstrated [5-7]. However, one critical native disadvantage of β -Ga₂O₃ is its extremely low thermal conductivity (k) (10~ 25 W/m·K) [8, 9], even compared with other popular wide bandgap semiconductors such as silicon carbide (SiC) at 387 W/m·K [10], aluminum nitride (AlN) at 200 W/m·K [11], and gallium nitride (GaN) at 170 W/m·K [12]. Because the applications above generate a significant amount of Joule heat during operation [13-15], a poor thermal property of β -Ga₂O₃ would become more pronounced in β -Ga₂O₃ based devices, which causes an even more increase in temperature and a nonuniform distribution of dissipated

power, thus emerging as one of the most serious concerns in the degradation of variability and reliability in β -Ga₂O₃ based applications. [16-18]

Since thermal management is critically important for the efficient operation of β -Ga₂O₃ based devices, several studies have been carried out to deal with the heat dissipation issue in β -Ga₂O₃. For example, Rimmon et al. [19] and A.O Nell et al. [20] reported a method of reducing the self-heating effect by straining silicon substrate and target material, leading to an increase in carrier mobility and thus balancing the effect of self-heat. However, this technology suffers two main challenges: it is difficult to control the defect densities between the interface of Si and target materials to control Si's strain relaxation levels. Another method by Li et al. [21, 22] and Shi et al. [21, 22] proposed a method of mitigating the low thermal conductivity issue, increasing the thermal boundary conductance, and lowering the thermal resistance of β -Ga₂O₃ with the assistance of metallic or dielectric interfacial layers. Recently, another novel route to manage a thermal property of β -Ga₂O₃ was reported by utilizing a sub-micron thin and freestanding format of β -Ga₂O₃, also called β -Ga₂O₃ nanomembrane (NM). β -Ga₂O₃ NMs can be transfer-printed

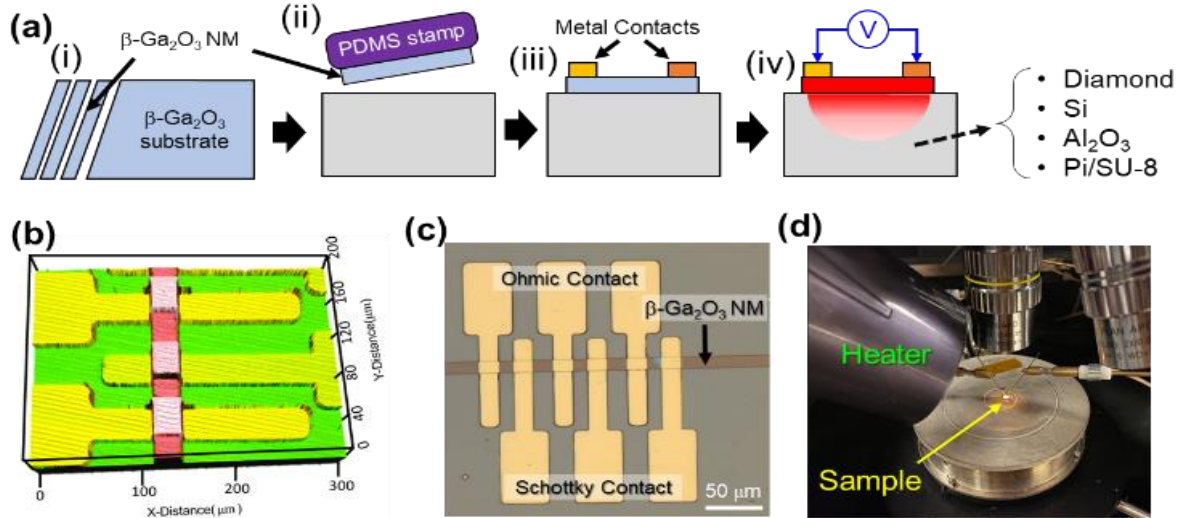


Figure 1. (a) A schematic illustration of the $\beta\text{-Ga}_2\text{O}_3$ NMs SBD fabrication process: (i) a creation of $\beta\text{-Ga}_2\text{O}_3$ NMs, (ii) a micro-transfer printing of $\beta\text{-Ga}_2\text{O}_3$ NMs onto four different substrates, (iii) a metallization on $\beta\text{-Ga}_2\text{O}_3$ NMs to form SBDs, (iv) a pulsed I-V characterization. (b) Three-dimensional morphology and (c) a microscopic image of the fabricated $\beta\text{-Ga}_2\text{O}_3$ NMs SBDs (d) an image of the heating setup.

onto any desired substrates. [23-26] Thus, efficient heat dissipation from $\beta\text{-Ga}_2\text{O}_3$ is expected when $\beta\text{-Ga}_2\text{O}_3$ NMs are transfer-printed on a high-k substrate. For example, Zheng et al. and Cheng et al. used single-crystal diamond substrate as a heat dissipator to create the $\beta\text{-Ga}_2\text{O}_3$ NM/diamond structure and successfully characterized the thermal conductivity of $\beta\text{-Ga}_2\text{O}_3$ NM and thermal boundary conductance at the $\beta\text{-Ga}_2\text{O}_3$ NM/diamond interface [8, 27, 28]. Cheng et al. and Yixiong et al. also formed $\beta\text{-Ga}_2\text{O}_3$ NM/SiC structure to realize a similar cooling effect. [29, 30] While all these studies on thermal management strategies on $\beta\text{-Ga}_2\text{O}_3$ provide insightful information about maximizing material property of $\beta\text{-Ga}_2\text{O}_3$, a comprehensive study on the impact of the electrical property on the heating effect depending on various substrates has not yet been experimentally demonstrated.

In this paper, $\beta\text{-Ga}_2\text{O}_3$ NMs based Schottky barrier diodes (SBDs) were formed on four different substrates via a micro-transfer printing that has a wide range of thermal conductivity from 0.25 W/m·K to 2200 W/m·K, which include polyimide, sapphire, silicon, and diamond substrate, and characterized a transport property of $\beta\text{-Ga}_2\text{O}_3$ NMs SBDs under different temperature conditions using a sub-micron second resolution time-resolved electrical measurement system. The devices exhibited noticeably less-delayed turn on/off transient time when $\beta\text{-Ga}_2\text{O}_3$ NMs SBDs were transfer-printed on a high-k substrate. Furthermore, a relationship between the $\beta\text{-Ga}_2\text{O}_3$ NM thicknesses and their time-resolved electrical properties was systematically investigated. We found that phonon scattering plays an important role in heat dissipation as the thickness of $\beta\text{-Ga}_2\text{O}_3$ NMs gets thinner, which is also verified by the Multiphysics simulator. Overall, our result reveals the

impact of various substrates with different thermal properties and different $\beta\text{-Ga}_2\text{O}_3$ NMs thickness with the performance of $\beta\text{-Ga}_2\text{O}_3$ NMs based devices. Hence, these results can guide future efforts to optimize the performance of future $\beta\text{-Ga}_2\text{O}_3$ devices by maximizing heat dissipation from the $\beta\text{-Ga}_2\text{O}_3$ layer.

2. Results and discussion

Figure 1(a) shows the schematic illustration of the device fabrication steps. The detail of the fabrication process can be found in the Experimental Section and Ref. [23-25, 31]. Briefly, the fabrication began with a $\beta\text{-Ga}_2\text{O}_3$ bulk substrate grown by molecular beam epitaxy and moderately Sn doped (concentration of $1 \times 10^{18} \text{ cm}^{-3}$). $\beta\text{-Ga}_2\text{O}_3$ NMs were created by a mechanical exfoliation method (Figure 1(a)(i)). Once $\beta\text{-Ga}_2\text{O}_3$ NMs were created, we carefully transfer-printed $\beta\text{-Ga}_2\text{O}_3$ NMs onto four different substrates using an elastomeric stamp (polydimethylsiloxane, PDMS); namely, undoped Si, sapphire, diamond, and polyimide (PI) substrates (Figure 1(a)(ii)). After completing the transfer process, an Ohmic metal stack and a Schottky metal stack were deposited to make Schottky barrier diodes (SBDs) (Figure 1(a)(iii)). Prior to Ohmic metal deposition, a plasma treatment was carried out on $\beta\text{-Ga}_2\text{O}_3$ NMs by a BCl_3/Ar plasma treatment using a reactive ion etcher (RIE) to achieve ohmic contact and avoid an additional high-temperature annealing process. Then, SBDs were measured using a Keithley 4200 SCS semiconductor parameter analyzer with a pulsed I-V unit in a dark box (Figure 1(a)(iv)). Figure 1(b) and (c) show the 3D

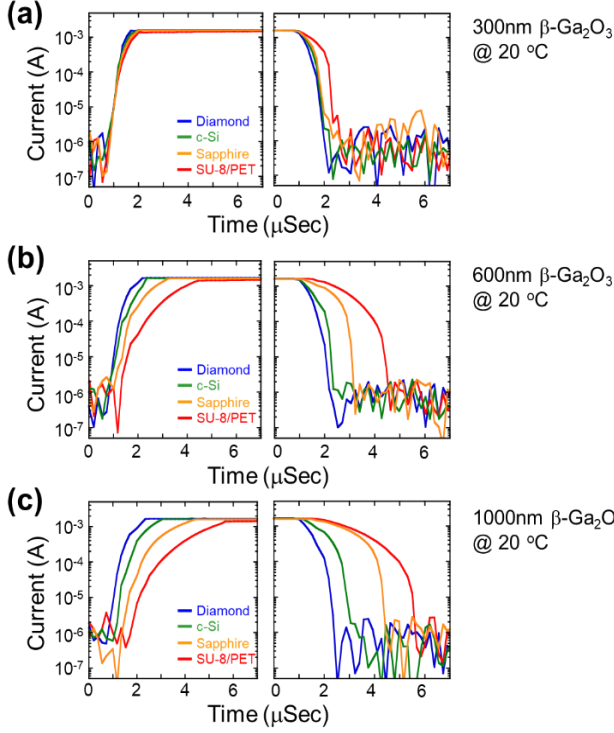


Figure 2. A set of pulsed I-V curves of $\beta\text{-Ga}_2\text{O}_3$ NM SBDs on four different substrates measured at room temperature with three different $\beta\text{-Ga}_2\text{O}_3$ NM thicknesses (a) 300 nm, (b) 600 nm, (c) 1000 nm, respectively.

profile and microscopic images of the as fabricated $\beta\text{-Ga}_2\text{O}_3$ NM SBDs on a diamond substrate to show a generic shape of $\beta\text{-Ga}_2\text{O}_3$ NM SBD. To compare transient time in $\beta\text{-Ga}_2\text{O}_3$ NM SBDs between room temperature and elevated temperature, the devices were exposed in heated air and incandescent lamp with the objective lens for 10 min to heat the top surface of the device, while the stainless-steel probe station stage remains at 20 °C as shown in Figure (d). Figure S1 shows I-V curves measured from $\beta\text{-Ga}_2\text{O}_3$ NM SBDs on PI, Si, sapphire, and diamond substrates with different $\beta\text{-Ga}_2\text{O}_3$ NM thicknesses varying from 300 nm to 1000 nm. All $\beta\text{-Ga}_2\text{O}_3$ NM SBDs exhibited a good rectifying behavior with an on/off ratio higher than 10^{-6} and the ideality factor (n) of 1.8 calculated based on thermionic emission theory [32]. The similarly good current-voltage (I-V) characteristics in $\beta\text{-Ga}_2\text{O}_3$ NM SBDs set a baseline for the time-resolved electrical characterization that relies on different substrates.

Compared with a typical direct current (DC) measurement, an investigation of transient time measurement using a pulsed I-V provides the isothermal condition of the device, thus offering a more accurate power dissipation effect and thermal resistance characteristics. Figure 2 shows the time-resolved pulsed I-V characteristics of the $\beta\text{-Ga}_2\text{O}_3$ NM SBDs on PI, Si, sapphire, and diamond substrates at room temperature. The devices were biased for 1 mSec with a current compliance of

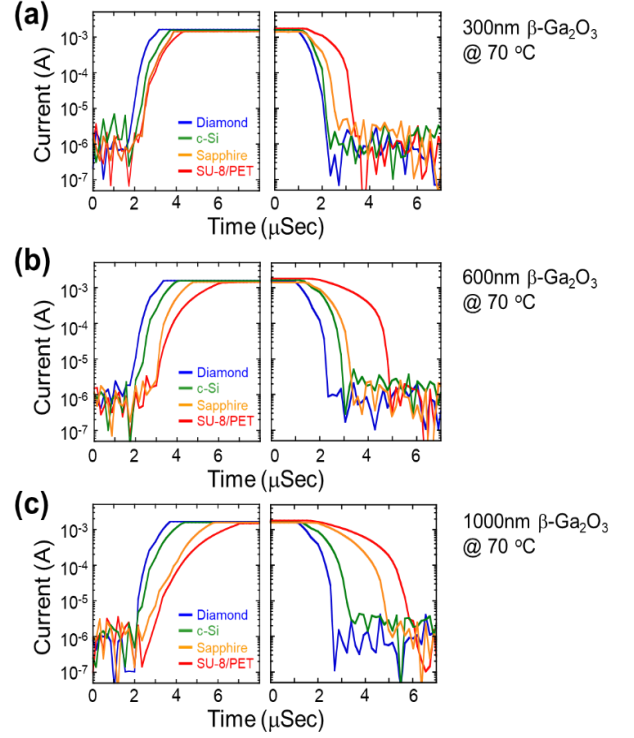


Figure 3. A set of pulsed I-V curves of $\beta\text{-Ga}_2\text{O}_3$ NM SBDs on four different substrates measured at 70 °C with three different Ga_2O_3 NM thicknesses (a) 300 nm, (b) 600 nm, (c) 1000 nm, respectively.

3 mA to prevent unwanted thermal damage. Details about the measurement setup can be found in the Method section. The left panel of Figure 2(a)-(c) are the zoom-in plots of transient rise times on different substrates and different $\beta\text{-Ga}_2\text{O}_3$ NM thicknesses (from 300 nm to 1000 nm). Similarly, the right panel of Figure 2(a)-(c) are the zoom-in plots of transient fall times on different substrates and the same $\beta\text{-Ga}_2\text{O}_3$ NM thicknesses, respectively. As shown in Figure 2, the rising and fall time of the devices are noticeably different depending on the substrate. $\beta\text{-Ga}_2\text{O}_3$ NM SBDs on diamond substrate show the shortest transient time, followed by the device with Si, sapphire, and PI substrate. The rising time for 300 nm thick $\beta\text{-Ga}_2\text{O}_3$ NM SBDs on the diamond, Si, sapphire, and PI substrates are measured to be 1.07 μs , 1.35 μs , 1.4 μs , and 2.65 μs , and their respective falling times are 1.07 μs , 1.5 μs , 1.65 μs , 2.85 μs , respectively. Interestingly, it was found that the falling time tends to be longer as $\beta\text{-Ga}_2\text{O}_3$ NM SBDs are built on the low-k substrate. The rising and fall time of $\beta\text{-Ga}_2\text{O}_3$ NM SBDs on diamond remained almost the same as 1.07 μs , while the fall time for devices on sapphire and PI substrate are increased than their rising from 1.4 μs and 2.65 μs to 1.65 μs and 2.85 μs , respectively. The trapping and de-trapping process in $\beta\text{-Ga}_2\text{O}_3$ NM and the interaction between $\beta\text{-Ga}_2\text{O}_3$ NM and substrate can explain this increase in the fall delay

characteristic. The trapping and de-trapping process in semiconductors refers to the electron recombining and releasing process to defects or vacancies. Considering that β -Ga₂O₃ has a high level of oxygen vacancies, the trapping and de-trapping process becomes one of the major sources of heat generation in β -Ga₂O₃ NMs. When β -Ga₂O₃ NM SBDs were biased, a Joule heat would be generated from the top surface of β -Ga₂O₃ NMs and begin to accumulate and propagate inside the β -Ga₂O₃ NM which is called a “self-heating” effect. This process supplies sufficient activation energy to overcome the trap potential barrier and escape from the trap by the equation (1) [33]:

$$J = n \frac{1}{\tau} \exp\left(-\frac{E_i}{kT}\right) \quad (1)$$

Also, the relationship between the trapping time and rising time can be determined by equation (2) [34]:

$$I = 1 - \exp\left(\frac{-t}{\tau}\right)^\beta \quad (2)$$

where J is the current density, τ is the trapping / de-trapping time constant, t is the trapping /de-trapping period, E_i is the trap energy, k is the Boltzmann constant, T is the temperature, I is the device on current, and β is the fitting parameter. When combining equations (1) and (2) with the same amount of the on-current, the traps with a shorter trapping time constant require shorter times to be filled. Due to the self-heating effect, as temperature increases, the trapping time constant increases and enables these traps to take longer time to be filled during the charging process. When devices were heated at the same rate and the input power to the device was the same, the rising time for each case did not vary noticeably. However, when the current is stopped, the heat must be dissipated both to air and substrate. The thermal conductivity values of diamond, Si, and sapphire are higher to 2200, 144, and 40 W/m·K, respectively than that of β -Ga₂O₃ NM, and the thermal conductivity of PI is substantially lower to 0.25 W/m·K than that of β -Ga₂O₃ NMs. [35-38] Thus, their cooling rates are different. As a result, we conclude that the switching characteristic becomes enhanced when β -Ga₂O₃ NMs SBDs are formed on a high- k substrate. This trend is consistent regardless of the thickness of β -Ga₂O₃ NMs (both 300 nm thick and 1000 nm thick β -Ga₂O₃ NMs), as shown in Figure 2.

To further investigate the relationship between delay time, devices substrates, and β -Ga₂O₃ NMs thickness, the same time-resolved pulsed I-V characterizations were performed at the elevated temperature. β -Ga₂O₃ NM SBDs were heated from two heating sources (namely, (1) a focused incandescent light bulb via an objective lens, (2) a heat gun) from the top of the device to heat the top surface of the device, not the bottom side of the substrate from the probe station stage because the typical stage heating method in the probe station heats the underneath of substrate, which affects devices differently depending on thermal conductivity of the substrate. Figure 3 shows the time-resolved pulsed I-V characteristics of the β -

Ga₂O₃ NMs SBDs on PI, Si, sapphire, and diamond substrates at elevated temperatures. The thermal imager was used to measure the surface temperature of β -Ga₂O₃ NMs SBDs. The devices were heated until the device temperature reaches 70 °C prior to the measurement and then biased at 3 mA for 1 mSec. In the left panel of Figure 3(a)-(c), the zoomed-in plots show the transient rise times on four different substrates and different β -Ga₂O₃ NM thicknesses. Similarly, the right panel of Figure 3(a)-(c) are the zoomed-in plots of transient fall times on four different substrates and different β -Ga₂O₃ NM thicknesses, respectively. The rising time for 300 nm thick β -Ga₂O₃ NMs SBDs on diamond, Si, sapphire, and PI substrates were 1.45 μ s, 1.55 μ s, 1.65 μ s, 3.4 μ s and their respective falling times are 1.45 μ s, 1.6 μ s, 1.8 μ s, and 3.8 μ s, respectively. Similar to the test result at room temperature, the rising and fall time of β -Ga₂O₃ NMs SBDs on diamond remained almost the same to be 1.45 μ s, while the fall time for devices on PI substrate was increased than their rising time

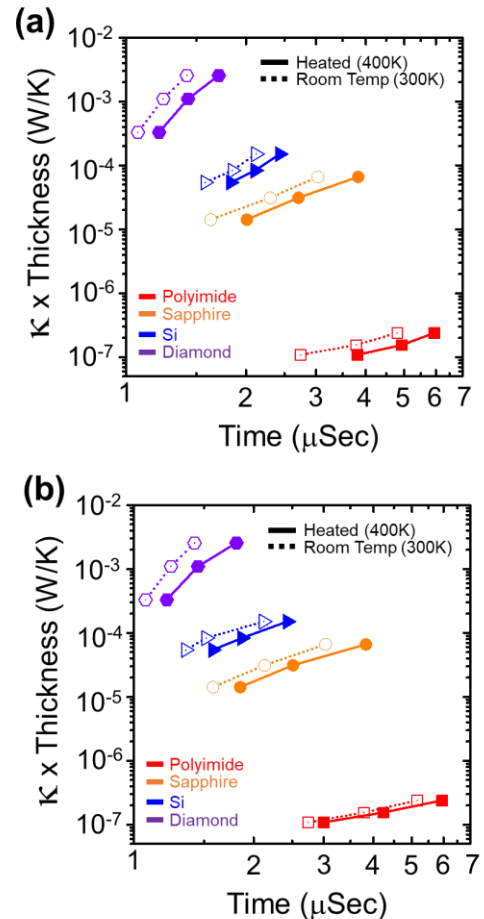


Figure 4. A summary of transient delay times of β -Ga₂O₃ NMs SBDs under four different substrates as a function of a product of thermal conductivity of the substrate and thickness of β -Ga₂O₃ NMs, (a) a rising delay times, (b) a fall delay times.

from 3.4 μ s to 3.8 μ s, respectively.

Figure 4(a) and (b) summarize the rising and fall time for $\beta\text{-Ga}_2\text{O}_3$ NM SBDs, respectively, which are extracted from Figure 2 and Figure 3. To provide a clear view of the relationship among the electrical performance of $\beta\text{-Ga}_2\text{O}_3$ NM SBDs with respect to the $\beta\text{-Ga}_2\text{O}_3$ NM thickness and thermal conductivity of the substrate, a transient delay time is plotted with the product of the $\beta\text{-Ga}_2\text{O}_3$ NM thickness and thermal conductivity of substrate (W/K·Sec: W/K vs. delay time). Therefore, the slope of the curve indicates the capacity of heat dissipation as well as the rate of the trapping/de-trapping process. For the rising time of $\beta\text{-Ga}_2\text{O}_3$ NM SBDs on the diamond substrate, the slope value is 6.32×10^{-3} which is 35, 168, and 1.02×10^4 times smaller than the one on Si, sapphire, and PI substrate, respectively. Similar trends were observed in the fall time of $\beta\text{-Ga}_2\text{O}_3$ NM SBDs on a diamond substrate compared with $\beta\text{-Ga}_2\text{O}_3$ NM SBDs on other substrates.

To further understand the heat dissipation effect on $\beta\text{-Ga}_2\text{O}_3$ NMs SBDs, we performed a Multiphysics simulation using the thermal module in COMSOL. The model structure was established using the same dimensional parameters and

references [8, 35-39]. In the simulation, the dissipated power was calculated as $P = V_{\text{on}} \times I_{\text{on}}$, where I_{on} is on state current and V_{on} is the corresponding bias. The actual biasing point was 3 mA at 4 V for all devices, thus an input power density of 12 mW was added to the electrode of the simulated structure. The initial temperature of the entire structure was set to 293.15 K as a boundary condition. Figure 5 and Figure S2 present the heat distribution of $\beta\text{-Ga}_2\text{O}_3$ NMs with 100 nm, 500 nm, and 1000 nm thicknesses under various substrates at the equilibrium state and the transit state at 1 μSec . As shown in Figure 5, the local temperature at the electrode/ $\beta\text{-Ga}_2\text{O}_3$ NM interface tends to rise higher when $\beta\text{-Ga}_2\text{O}_3$ NMs SBDs are on a lower-k substrate. The interface temperature of $\beta\text{-Ga}_2\text{O}_3$ NMs SBDs on the diamond, Si, sapphire, and PI substrate under the biasing condition were calculated to be 298 K, 334 K, 365 K, and 420 K, respectively, which suggests that efficient heat dissipation can occur, or the higher power can be handled when $\beta\text{-Ga}_2\text{O}_3$ devices are built on a high-k substrate. In addition, the heat distributions of various thick- $\beta\text{-Ga}_2\text{O}_3$ NMs on different substrates were simulated.

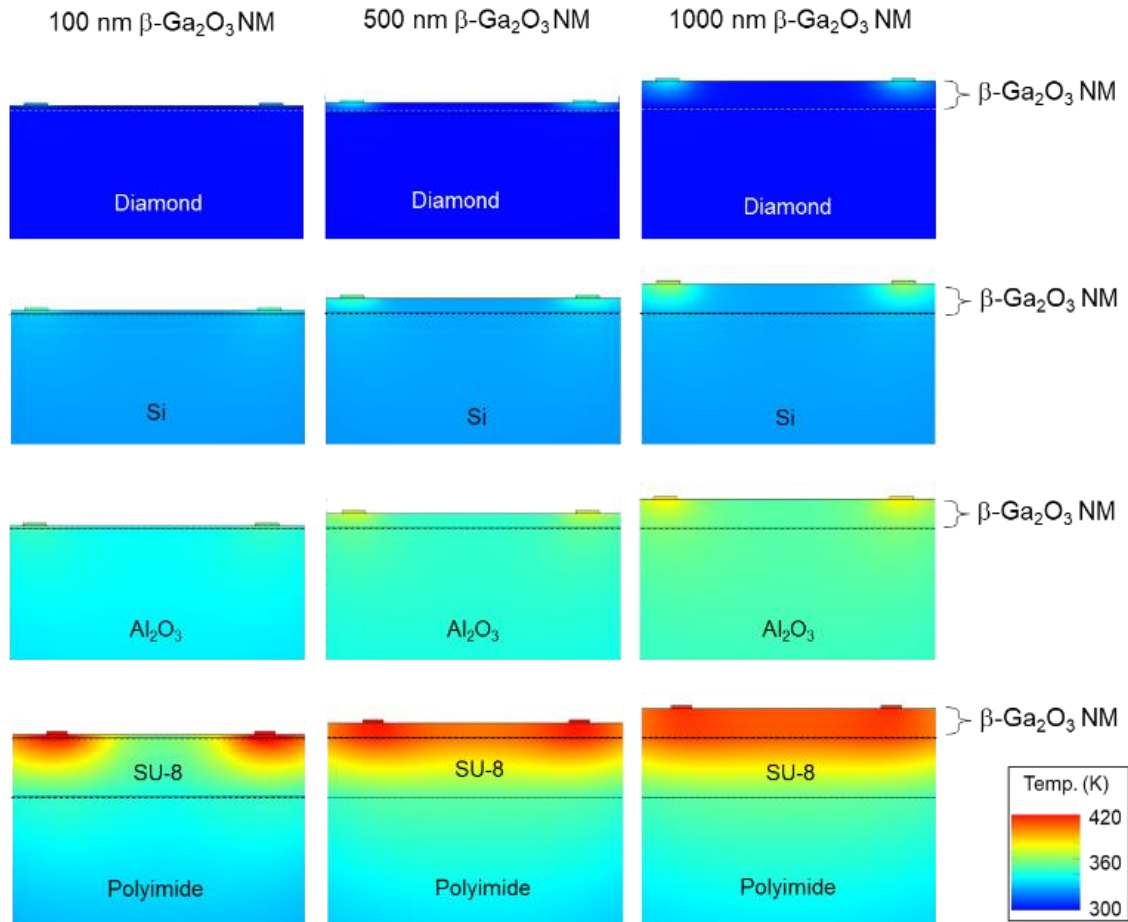


Figure 5. Simulated temperature profiles of $\beta\text{-Ga}_2\text{O}_3$ NMs on four different substrates and three different $\beta\text{-Ga}_2\text{O}_3$ NM thicknesses.

the empirical material parameters such as density, crystal structure, thermal resistance, and heat capacity from various

Each row from the left to right of Figure 5 shows the simulation result with 100 nm, 500 nm, and 1000 nm thick $\beta\text{-Ga}_2\text{O}_3$ NMs on different substrates.

Table 1. Thermal conductivity values of substrates and β -Ga₂O₃ used in the simulation.

	TC
PI ^[35]	0.25 W/m·K
SU-8 ^[36]	0.2 W/m·K
Si ^[37]	144 W/m·K
Sapphire ^[38]	40 W/m·K
Diamond ^[39]	2200 W/m·K
β -Ga ₂ O ₃ NM ^[8]	3.1 W/m·K (100 nm), 5.2 W/m·K (500 nm), 8.68 W/m·K (1000 nm)

Ga₂O₃ NM on different substrates. In this simulation, we used the empirical thermal conductivity values of β -Ga₂O₃ NM by Yixiong et al. and Zheng et al. [8, 27], which shows a decreasing trend in thermal conductivity of β -Ga₂O₃ NM from 8.7 W/m·K for 1000 nm thick β -Ga₂O₃ NM to 3.1 W/m·K for 100 nm thick β -Ga₂O₃ NM. As thermal conductivity becomes smaller as the thickness of β -Ga₂O₃ NM decreases, one could expect to see a higher temperature in β -Ga₂O₃ NM as the thickness of β -Ga₂O₃ NMs decrease. However, the simulation result revealed that the electrode/ β -Ga₂O₃ NM interface temperature decreases as the thickness of β -Ga₂O₃ NM decreases. While it is true that the thermal conductivity of thinner β -Ga₂O₃ NM is smaller than the thicker one (i.e., 8.7 W/m·K for 1000 nm thick β -Ga₂O₃ NM and 3.1 W/m·K for 100 nm thick β -Ga₂O₃ NM) thus β -Ga₂O₃ NMs are prone to be heated as β -Ga₂O₃ NMs get thinner, faster heat dissipation could occur when β -Ga₂O₃ NMs are thinner and built on a high-k substrate. The simulation result suggests that the devices with a thin β -Ga₂O₃ NM can dissipate heat faster through a high-k substrate which is critically important to prevent the device from overheating during a biasing condition. However, the opposite trend was observed in the case of β -Ga₂O₃ NM SBDs on PI substrate which represents a low-k substrate. In other words, the temperature at the electrode/ β -Ga₂O₃ NM interface gets heated several tens of degrees higher to 405 K, 413 K, and 420 K as the thickness of β -Ga₂O₃ NM is reduced from 1000 nm to 500 nm and 100 nm, respectively. This opposite trend can be explained by the thermal conductivity of β -Ga₂O₃ NM and PI substrate. As shown in Table 1, the thermal conductivity of β -Ga₂O₃ NMs (5 W/m·K on average) is much larger than the thermal conductivity of PI and SU-8 (0.25 and 0.2 W/m·K, respectively). Thus, heat dissipation occurs along with the β -Ga₂O₃ NM, rather than through the PI substrate. Therefore, as the simulation result indicates, the integration of β -Ga₂O₃ NM with a low-k substrate degrades the contact resistance and affects the sheet resistance and overall bulk properties.

3. Conclusions

In conclusion, a transient delayed rising and fall time of β -Ga₂O₃ NMs SBDs formed on four different substrates were measured using a sub-micron second resolution time-resolved electrical measurement system under a different temperature condition. The devices exhibited noticeably less-delayed turn on/off transient time when β -Ga₂O₃ NMs SBDs were transfer-printed on a high-k substrate. Furthermore, a relationship between the β -Ga₂O₃ NM thicknesses and their time-resolved electrical properties was systematically investigated and found that phonon scattering plays an important role in heat dissipation as the thickness of β -Ga₂O₃ NMs get thinner which is also verified by the Multiphysics simulator. Overall, our result reveals the impact of various substrates with different thermal properties and different β -Ga₂O₃ NMs thickness with the performance of β -Ga₂O₃ NMs based devices. Hence, these results can guide further efforts us to optimize the performance of future β -Ga₂O₃ devices by maximizing heat dissipation from the β -Ga₂O₃ layer.

4. Experimental Section

4.1 Device fabrication process

The fabrication process began with a β -Ga₂O₃ bulk substrate grown by molecular beam epitaxy and moderately Sn doped (concentration of 1×10^{18} cm⁻³) on the [201] direction. The β -Ga₂O₃ NMs were created by clipping several large segments from the bulk substrate at an angle of 77°, followed by an exfoliation using a well-known taping method. β -Ga₂O₃ segments were easily mechanically exfoliated in [100] direction due to the weak binding energy in this direction. [23-25, 31] In this step, various thicknesses β -Ga₂O₃ nanomembranes can be created by adjusting exfoliation times. Once β -Ga₂O₃ NMs were created, we carefully transfer printed them onto undoped Si, sapphire, diamond, and SU-8 coated polyimide substrates by using an elastomeric stamp (polydimethylsiloxane, PDMS). Prior to the transfer, all the substrates were cleaned thoroughly by the sonification process in acetone, isopropyl alcohol, and DI water for 10 min in each step. After completion of the transfer processes, Ohmic metal and Schottky metal electrodes deposition processes were conducted. Prior to Ohmic metal deposition, a plasma treatment was carried out on β -Ga₂O₃ NMs by a BCl₃/Ar plasma treatment using a reactive ion etcher (RIE) to achieve ohmic contact and to avoid an additional high-temperature annealing process. After that, an Ohmic metal stack (Ti/Au = 20/100 nm) and a Schottky metal stack (Ti/Pt/Au = 20/30/100 nm) were deposited to complete the fabrication of the device.

4.2 Measurement setup

The electrical characterization was carried out using a Keithley 4200 semiconductor parameter analyzer. The voltage-current measurement was conducted at voltage bias -4 V to 4 V. To analyze the heat dissipation effect of β -Ga₂O₃

NMs based diodes, the pulsed I-V setup was implemented as follows: the anode bias is pulsed from off state to on state. The pulse width was 500 μ s with a pulse period of 1000 μ s. The time resolution of a rise and fall time of pulsed I-V unit was 0.17 μ Sec. And all devices were measured with the current compliance setting at 3 mA

Data availability statement

The data that support the findings of this study are available upon reasonable request from the authors.

Acknowledgements

This work was supported by the National Science Foundation (Grant number: ECCS-1809077).

References

- [1] Sharma S, Zeng K, Saha S and Singiseti U 2020 Field-Plated Lateral Ga₂O₃ MOSFETs With Polymer Passivation and 8.03 kV Breakdown Voltage *IEEE Electron Device Lett.* **41** 836-9.
- [2] Hasan M N, Swinnich E and Seo J-H *Wide Bandgap Semiconductor Electronics and Devices*, pp 63-78.
- [3] Pearton S J, Yang J, Cary P H, Ren F, Kim J, Tadjer M J and Mastro M A 2018 A review of Ga₂O₃ materials, processing, and devices *Appl. Phys. Rev.* **5** 011301.
- [4] Higashiwaki M, Sasaki K, Kuramata A, Masui T and Yamakoshi S 2012 Gallium oxide (Ga₂O₃) metal-semiconductor field-effect transistors on single-crystal β -Ga₂O₃ (010) substrates *Appl. Phys. Lett.* **100** 013504.
- [5] Zeng K, Vaidya A and Singiseti U 2019 A field-plated Ga₂O₃ MOSFET with near 2-kV breakdown voltage and 520 ohm·cm² on-resistance *Appl. Phys. Express* **12** 081003.
- [6] Green A J, Chabak K D, Baldini M, Moser N, Gilbert R, Fitch R C, Wagner G, Galazka Z, Mccandless J, Crespo A, Leedy K and Jessen G H 2017 β -Ga₂O₃ MOSFETs for Radio Frequency Operation *IEEE Electron Device Lett.* **38** 790-3.
- [7] Oh S, Kim C-K and Kim J 2018 High Responsivity β -Ga₂O₃ Metal-Semiconductor-Metal Solar-Blind Photodetectors with Ultraviolet Transparent Graphene Electrodes *ACS Photonics* **5** 1123-8.
- [8] Zheng Y, Swinnich E and Seo J-H 2020 Investigation of Thermal Properties of β -Ga₂O₃ Nanomembranes on Diamond Heterostructure Using Raman Thermometry *ECS J. Solid State Sci. Technol.* **9** 055007.
- [9] Guo Z, Verma A, Wu X, Sun F, Hickman A, Masui T, Kuramata A, Higashiwaki M, Jena D and Luo T 2015 Anisotropic thermal conductivity in single crystal β -gallium oxide *Appl. Phys. Lett.* **106** 111909.
- [10] Burgemeister E A, Muench W v and Pettenpaul E 1979 Thermal conductivity and electrical properties of 6H silicon carbide *J. Appl. Phys.* **50** 5790-4.
- [11] Jackson T B, Virkar A V, More K L, Dinwiddie Jr. R B and Cutler R A 1997 High-Thermal-Conductivity Aluminum Nitride Ceramics: The Effect of Thermodynamic, Kinetic, and Microstructural Factors *J. Am. Ceram. Soc.* **80** 1421-35.
- [12] Zou J, Kotchetkov D, Balandin A A, Florescu D I and Pollak F H 2002 Thermal conductivity of GaN films: Effects of impurities and dislocations *J. Appl. Phys.* **92** 2534-9.
- [13] Pearton S J, Ren F, Tadjer M and Kim J 2018 Perspective: Ga₂O₃ for ultra-high power rectifiers and MOSFETS *J. Appl. Phys.* **124** 220901.
- [14] Sharma R, Patrick E, Law M E, Yang J, Ren F and Pearton S J 2019 Thermal Simulations of High Current β -Ga₂O₃ Schottky Rectifiers *ECS J. Solid State Sci. Technol.* **8** Q3195-Q201.
- [15] Zhou H, Maize K, Qiu G, Shakouri A and Ye P D 2017 β -Ga₂O₃ on insulator field-effect transistors with drain currents exceeding 1.5 A/mm and their self-heating effect *Appl. Phys. Lett.* **111** 092102.
- [16] Liu S E, Wang J S, Lu Y R, Huang D S, Huang C F, Hsieh W H, Lee J H, Tsai Y S, Shih J R, Lee Y H and Wu K 2014 Self-heating effect in FinFETs and its impact on devices reliability characterization. In: 2014 IEEE International Reliability Physics Symposium, pp 4A..1-4A.
- [17] Semenov O, Vassighi A and Sachdev M 2006 Impact of self-heating effect on long-term reliability and performance degradation in CMOS circuits *IEEE Trans. Device Mater. Rel.* **6** 17-27.
- [18] Benbakhti B, Soltani A, Kalna K, Rousseau M and Jaeger J D 2009 Effects of Self-Heating on Performance Degradation in AlGa_N/Ga_N-Based Devices *IEEE Trans. Electron Devices.* **56** 2178-85.
- [19] Agaiby R, Yang Y, Olsen S H, O'Neill A G, Eneman G, Verheyen P, Loo R and Claeys C 2007 Quantifying self-heating effects with scaling in globally strained Si MOSFETs *Solid State Electron.* **51** 1473-8.
- [20] O'Neill A, Agaiby R, Olsen S, Yang Y, Hellstrom P E, Ostling M, Oehme M, Lyutovich K, Kasper E, Eneman G, Verheyen P, Loo R, Claeys C, Fiegna C and Sangiorgi E 2008 Reduced self-heating by strained silicon substrate engineering *Appl. Surf. Sci.* **254** 6182-5.
- [21] Li X, Park W, Wang Y, Chen Y P and Ruan X 2019 Reducing interfacial thermal resistance between metal and dielectric materials by a metal interlayer *J. Appl. Phys.* **125** 045302.
- [22] Shi J, Yuan C, Huang H-L, Johnson J, Chae C, Wang S, Hanus R, Kim S, Cheng Z, Hwang J and Graham S 2021

- Thermal Transport across Metal/ β -Ga₂O₃ Interfaces *ACS Appl. Mater. Interfaces* **13** 29083-91.
- [23] Lai J, Hasan M N, Swinnich E, Tang Z, Shin S-H, Kim M, Zhang P and Seo J-H 2020 Flexible crystalline β -Ga₂O₃ solar-blind photodetectors *J. Mater. Chem. C* **8** 14732-9.
- [24] Swinnich E, Hasan M N, Zeng K, Dove Y, Singiseti U, Mazumder B and Seo J-H 2019 Flexible β -Ga₂O₃ Nanomembrane Schottky Barrier Diodes *Adv. Electron. Mater.* **5** 1800714.
- [25] Hasan M N, Lai J, Swinnich E, Zheng Y, Baboukani B S, Nalam P C and Seo J-H 2021 Flexible Electronics: Investigation of Nano-Gaps in Fractured β -Ga₂O₃ Nanomembranes Formed by Uniaxial Strain *Adv. Electron. Mater.* **7** 2170006.
- [26] Kim M, Seo J-H, Singiseti U and Ma Z 2017 Recent advances in free-standing single crystalline wide band-gap semiconductors and their applications: GaN, SiC, ZnO, β -Ga₂O₃, and diamond *J. Mater. Chem. C* **5** 8338-54.
- [27] Zheng Y and Seo J-H 2020 A simplified method of measuring thermal conductivity of β -Ga₂O₃ nanomembrane *Nano Express* **1** 030010.
- [28] Cheng Z, Yates L, Shi J, Tadjer M J, Hobart K D and Graham S 2019 Thermal conductance across β -Ga₂O₃-diamond van der Waals heterogeneous interfaces *APL Mater.* **7** 031118.
- [29] Zheng Y, Feng Z, Bhuiyan A F M A U, Meng L, Dhole S, Jia Q, Zhao H and Seo J-H 2021 Large-size free-standing single-crystal β -Ga₂O₃ membranes fabricated by hydrogen implantation and lift-off *J. Mater. Chem. C* **9** 6180-6.
- [30] Cheng Z, Mu F, You T, Xu W, Shi J, Liao M E, Wang Y, Huynh K, Suga T, Goorsky M S, Ou X and Graham S 2020 Thermal Transport across Ion-Cut Monocrystalline β -Ga₂O₃ Thin Films and Bonded β -Ga₂O₃-SiC Interfaces *ACS Appl. Mater. Interfaces* **12** 44943-51.
- [31] Zheng Y, Hasan M N and Seo J-H 2021 High-Performance Solar Blind UV Photodetectors Based on Single-Crystal Si/ β -Ga₂O₃ p-n Heterojunction *Adv. Mater. Technol.* **6** 2100254.
- [32] Herring C and Nichols M H 1949 Thermionic Emission *Rev. Mod. Phys.* **21** 185-270.
- [33] Woo H and Jeon S 2017 Microsecond Pulse I-V Approach to Understanding Defects in High Mobility Bilayer Oxide Semiconductor Transistor *Sci. Rep.* **7** 8235.
- [34] Meneghesso G, Meneghini M, Bisi D, Rossetto I, Cester A, Mishra U K and Zanoni E 2013 Trapping phenomena in AlGaIn/GaN HEMTs: a study based on pulsed and transient measurements *Semicond. Sci. Technol.* **28** 074021.
- [35] Zhou H, Maize K, Noh J, Shakouri A and Ye P D 2017 Thermodynamic Studies of β -Ga₂O₃ Nanomembrane Field-Effect Transistors on a Sapphire Substrate *ACS Omega* **2** 7723-9.
- [36] Glassbrenner C J and Slack G A 1964 Thermal Conductivity of Silicon and Germanium from 30K to the Melting Point *Phys. Rev.* **134** A1058-A69.
- [37] Wang T, Wang M, Fu L, Duan Z, Chen Y, Hou X, Wu Y, Li S, Guo L, Kang R, Jiang N and Yu J 2018 Enhanced Thermal Conductivity of Polyimide Composites with Boron Nitride Nanosheets *Sci. Rep.* **8** 1557.
- [38] Sukhadolau A V, Ivakin E V, Ralchenko V G, Khomich A V, Vlasov A V and Popovich A F 2005 Thermal conductivity of CVD diamond at elevated temperatures *Diam. Relat. Mater.* **14** 589-93.
- [39] Oh S H, Lee K-C, Chun J, Kim M and Lee S S 2001 Micro heat flux sensor using copper electroplating in SU-8 microstructures *J. Micromech. Microeng.* **11** 221-5

Supplementary Information

for

Transient Characteristics of β -Ga₂O₃ Nanomembrane Schottky Barrier
Diodes on Various Substrates

by

*Junyu Lai, Jung-Hun Seo**

Department of Materials Design and Innovation,
University at Buffalo, The State University of New York,
Buffalo, NY USA 14260

*Email: junghuns@buffalo.edu

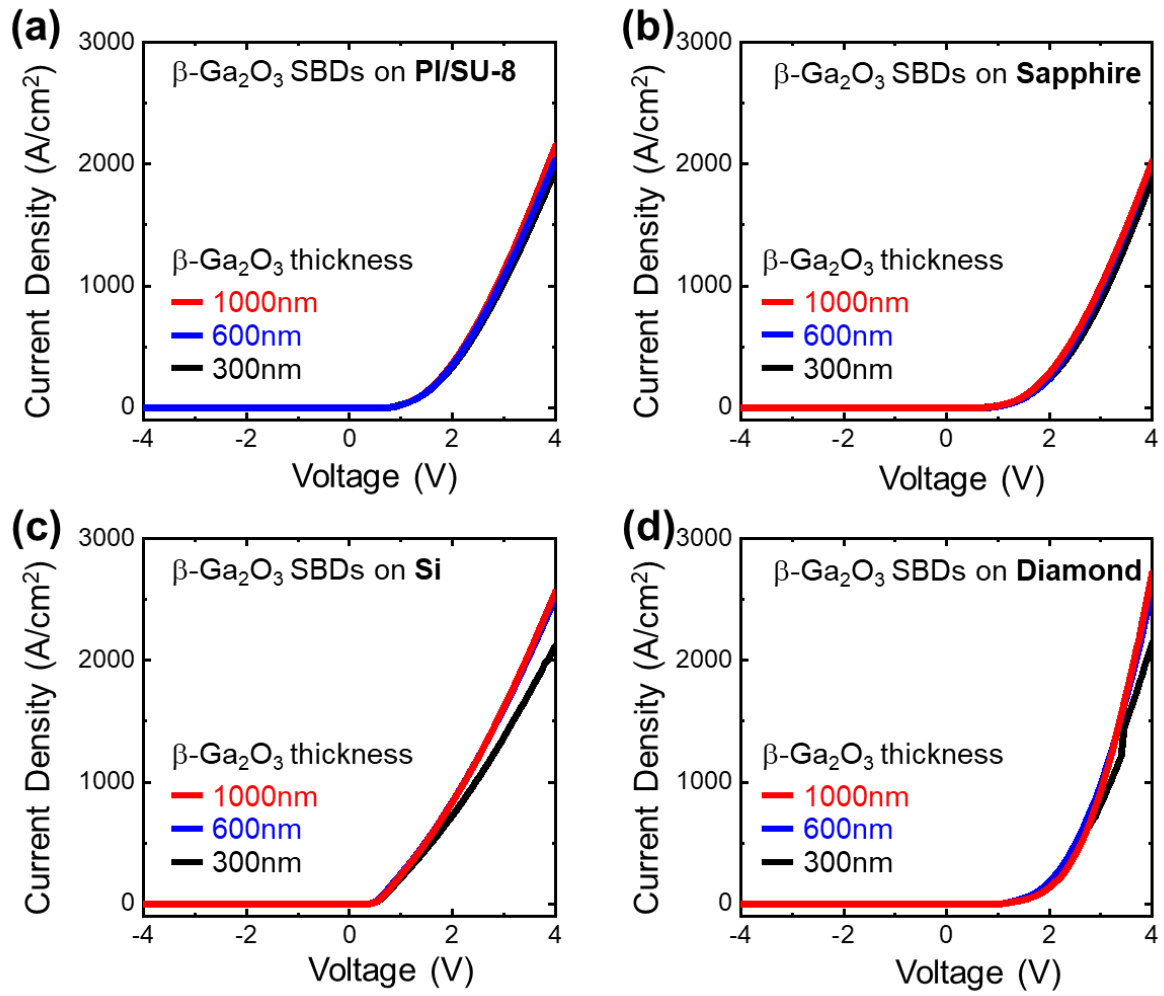


Figure S1. I-V characteristics of β -Ga₂O₃ NM SBDs with various NM thicknesses on (a) PI, (b) Si, (c) sapphire, and (d) diamond substrates at -4V to 4V.

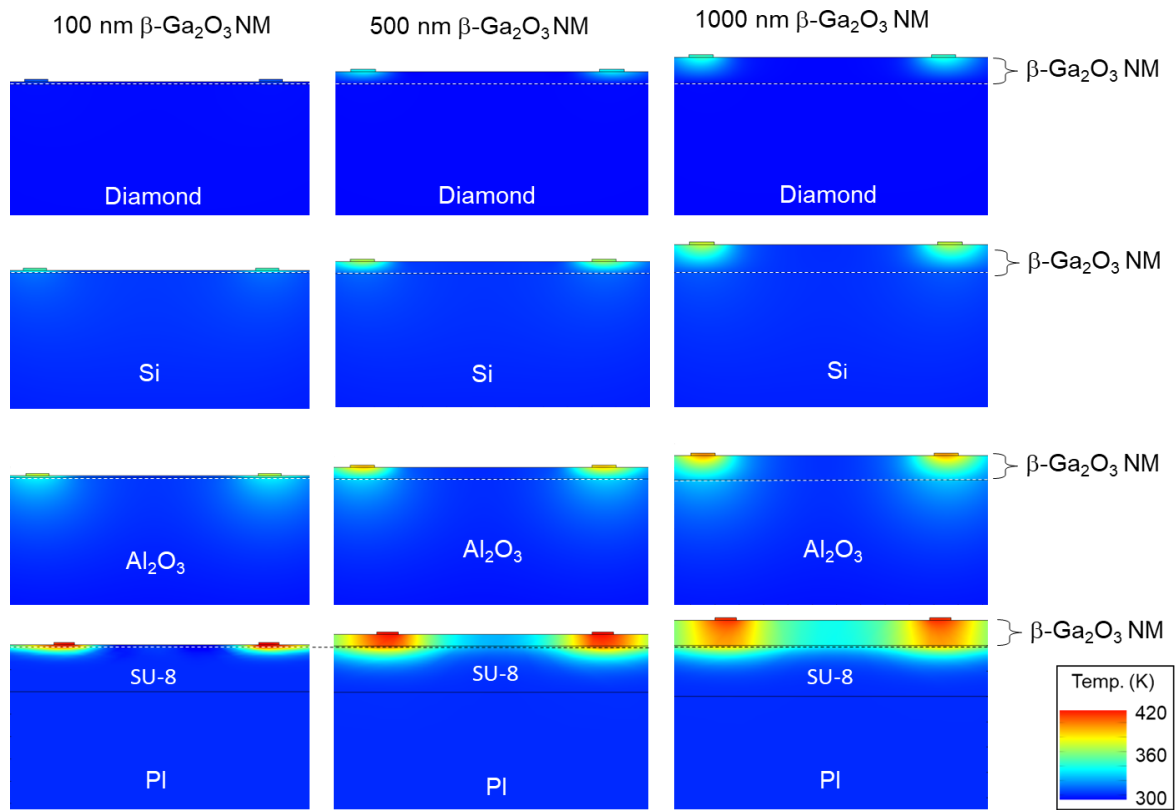


Figure S2. Simulated transient temperature profiles ($P=0.01$ W, $t=0.01$ s) of β -Ga₂O₃ NMs with (a) 100 nm, (b) 500 nm, and (c) 1000 nm thickness, on (i) diamond, (ii) Si, (iii) sapphire, and (iv) PI substrates.